



HAL
open science

Time-resolved piezoelectric response in relaxor ferroelectric $(\text{Pb}_{0.88}\text{La}_{0.12})(\text{Zr}_{0.52}\text{Ti}_{0.48})\text{O}_3$ thin films

Matthias Rössle, Olivier Thomas, Cristian Mocuta, Raphael Rousset, Michael Texier, Stéphanie Escoubas, Catherine Dubourdieu, Eudes B Araújo, Thomas W Cornelius

► To cite this version:

Matthias Rössle, Olivier Thomas, Cristian Mocuta, Raphael Rousset, Michael Texier, et al.. Time-resolved piezoelectric response in relaxor ferroelectric $(\text{Pb}_{0.88}\text{La}_{0.12})(\text{Zr}_{0.52}\text{Ti}_{0.48})\text{O}_3$ thin films. Journal of Applied Physics, 2022, 10.1063/5.0077785 . hal-03572696

HAL Id: hal-03572696

<https://hal.science/hal-03572696>

Submitted on 14 Feb 2022

HAL is a multi-disciplinary open access archive for the deposit and dissemination of scientific research documents, whether they are published or not. The documents may come from teaching and research institutions in France or abroad, or from public or private research centers.

L'archive ouverte pluridisciplinaire **HAL**, est destinée au dépôt et à la diffusion de documents scientifiques de niveau recherche, publiés ou non, émanant des établissements d'enseignement et de recherche français ou étrangers, des laboratoires publics ou privés.

Time-resolved piezoelectric response in relaxor ferroelectric

$(\text{Pb}_{0.88}\text{La}_{0.12})(\text{Zr}_{0.52}\text{Ti}_{0.48})\text{O}_3$ thin films

Matthias Rössle¹, Olivier Thomas², Cristian Mocuta³, Raphael Rousset², Michael Texier², Stéphanie Escoubas², Catherine Dubourdieu^{4,5}, Eudes B. Araújo⁶, Thomas W. Cornelius^{2*}

¹ Helmholtz-Zentrum Berlin für Materialien und Energie GmbH, Wilhelm-Conrad Röntgen Campus, BESSY II, Albert-Einstein-Straße 15, 12489 Berlin, Germany

² Aix Marseille Univ, Univ Toulon, CNRS, IM2NP UMR 7334, Marseille, France

³ Synchrotron SOLEIL, L'Orme des Merisiers, Saint-Aubin - BP 48, 91192 Gif-sur-Yvette Cedex, France

⁴ Institute Functional Oxides for Energy-Efficient Information Technology, Helmholtz-Zentrum Berlin für Materialien und Energie GmbH, Hahn-Meitner-Platz 1, 14109 Berlin, Germany

⁵ Freie Universität Berlin, Physical Chemistry, Arnimallee 22, 14195 Berlin, Germany

⁶ São Paulo State University (UNESP), School of Natural Sciences and Engineering, Department of Physics and Chemistry, 15385-000 Ilha Solteira, SP, Brazil

**Corresponding author*

Thomas W. Cornelius

IM2NP UMR 7334 CNRS

Aix-Marseille Université

Faculté des Sciences, Campus de St Jérôme - Case 262

Avenue Escadrille Normandie Niemen

13397 Marseille Cedex 20

France

Email: thomas.cornelius@im2np.fr

This is the author's peer reviewed, accepted manuscript. However, the online version of record will be different from this version once it has been copyedited and typeset.
PLEASE CITE THIS ARTICLE AS DOI: 10.1063/1.50077785

Abstract

The domain switching dynamics in a relaxor ferroelectric lanthanum modified lead zirconate titanate thin film with 12 mol% La was investigated by time-resolved X-ray diffraction. While most frequently epitaxial thin films are investigated, the present work reports results on a polycrystalline thin film. Asymmetric butterfly loops of the strain as a function of the applied electric field evidenced a built-in electric field oriented towards the thin film-substrate interface. The piezoelectric coefficient d_{33} (in the film reference frame) diminishes with the increasing frequency of an applied AC electric field. From the strain transient during the application of Positive-Up Negative-Down voltage pulse sequences with frequencies of up to 100 kHz, characteristic times of the order of 100 to 200 ns were determined for these relaxor ferroelectric thin films. While switching times ranging from the picosecond to the millisecond range are reported in the literature for different materials, these characteristic switching times are comparable to epitaxial PZT thin films of various compositions despite the polycrystallinity of the present thin film. However, the evidenced built-in electric field significantly influences the switching behavior for different polarities.

Introduction

Piezo transducers based on piezoelectric materials are used to convert electrical energy into mechanical energy and *vice-versa*. They are widely used in communication, sensing, and energy harvesting applications. Piezoelectric materials are thus integrated into the various present and future commercial devices, including resonators, actuators, and sensors. Due to the need to minimize the size of consumer devices, thin-film structures are necessary for the integration into microelectronics [1]. It is well established that the piezoelectric coupling coefficients are very large in crystalline materials that are also ferroelectric, *i.e.* which exhibit a remnant electrical polarization, switchable by applying an external electric field. For commercial applications, especially in sensing and switching devices like piezo-actuators [2,3], the reliable and fast response to the external electrical field is important.

Lead-zirconate titanate (PZT) is probably one of the most studied ferroelectric materials, especially due to its excellent dielectric and piezoelectric properties. The interest in this system for compositions near the so-called morphotropic phase boundary (MPB) with the Zr/Ti compositional ratio around 52/48 is still large. Here, the presence of a monoclinic C_m phase enhances the piezoelectric response of PZT [4,5]. The ferroelectric properties of PZT can be improved by chemical substitution with different ions such as Na or Nd [6]. For instance, substituting Pb^{3+} with La^{3+} ions distorts the unit cell and decreases the oxygen vacancy concentration leading to a transition from a normal ferroelectric to a relaxor ferroelectric as the La content is increased [7]. Since its discovery in 1971, lanthanum-modified PZT (PLZT) relaxor ferroelectric compositions have been studied in thin-film structures as promising candidates for various applications. Among them, their high relative permittivity, spontaneous polarization, and lower leakage currents justify their application in non-volatile memories [8]. While the physical properties of ordinary ferroelectrics are well described by the Ginzburg-Landau-Devonshire theory [9], relaxor ferroelectrics escape a simple physical description. The characteristic physical properties of relaxors such as large dielectric permittivity and domain switching are often associated with polar nanoregions so that a local polar order develops, but no long-range order is observed [10,11,12,13,14]. However, despite enormous experimental and theoretical efforts [15], no

theoretical model exists to describe the diffuse phase transition and the large temperature and frequency-dependent dielectric maximum. In addition to the classical relaxor composition $(\text{Pb}_{0.91}\text{La}_{0.09})(\text{Zr}_{0.65}\text{Ti}_{0.35})\text{O}_3$ (PLZT 9/65/35), explored in the last 50 years due to its potential in optoelectronics, microelectronics, and electromechanics [16], other compositions have also been studied. The $(\text{Pb}_{0.88}\text{La}_{0.12})(\text{Zr}_{0.52}\text{Ti}_{0.48})\text{O}_3$ (PLZT 12/52/48) composition studied in the present work also exhibits a relaxor behavior and has been explored due to its optoelectronic properties such as the photovoltaic effect [17].

The piezoelectric properties of ferroelectric thin films are studied by various methods, including piezoresponse force microscopy (PFM), interferometry [18], and *in situ* and time-resolved X-ray diffraction (XRD) during the application of an electric field [19,20,21,22,23,24,25,26,27]. While PFM is a local probe and prone to surface artifacts, XRD provides access to the piezoelectrically-induced strain within the complete thickness of the thin film and on a large lateral scale with a strain resolution of 10^{-4} . In addition, X-ray diffraction allows for probing the piezoelectric anisotropy by measuring various Bragg reflections, thus exploring different lattice planes. *In situ* XRD has successfully been employed to study domain switching [28], imprint effect [29] as well as the structural evolution during imprint [30]. Moreover, time-resolved X-ray diffraction provides access to the temporal response and relaxation of the piezoelectrically-induced strain during actuation [31]. Most of the results on *in situ* and time-resolved X-ray diffraction reported in literature actually focus on epitaxial thin films and single crystals. However, very few studies using the aforementioned techniques concentrate on polycrystalline thin films.

In the present study, a polycrystalline relaxor ferroelectric PLZT 12/52/48 thin film was investigated by time-resolved synchrotron X-ray diffraction. These studies built on *in situ* X-ray diffraction during the application of DC and AC voltages revealing asymmetric butterfly loops of the piezoelectrically-induced strain as a function of the applied electric field, which evidence a built-in electric field in the thin film, which is oriented from the top electrode towards the bottom electrode [32]. Applying PUND (Positive-Up Negative-Down) pulse sequences with frequencies ranging from 15

to 100 kHz, the strain response was analyzed by time-resolved X-ray diffraction with a temporal resolution of about 100 ns.

Experimental

Lanthanum-modified lead zirconate titanate ($\text{Pb}_{0.88}\text{La}_{0.12}$)($\text{Zr}_{0.52}\text{Ti}_{0.48}$) O_3 (denoted in the following as PLZT12) thin films were prepared by the acetate solution route [32]. The solution was prepared by sequentially adding stoichiometric zirconium butoxide $\text{Zr}(\text{OC}_4\text{H}_9)_4$ (Aldrich 80%), titanium isopropoxide $\text{C}_{12}\text{H}_{28}\text{O}_4\text{Ti}$ (Fluka), lead acetate $(\text{CH}_3\text{COO})_2\text{Pb}\cdot 3\text{H}_2\text{O}$ (Dinâmica), and lanthanum oxide La_2O_3 (Aldrich) precursors. The titanium isopropoxide was added into a beaker containing zirconium butoxide at room temperature under stirring for 5 min. Then, 1 mL of glacial acetic acid was added at room temperature under stirring for another 5 min. Finally, lead acetate and lanthanum oxide were added to the solution while heating it to 80 °C on a hot plate. After completing the solubilization by adding 2 mL of acetic acid and 1 mL of distilled water (~20 min) the solution was cooled down to room temperature while stirring until a completely transparent and stable solution (0.4 M) was obtained.

PLZT12 thin films were deposited on Pt/TiO₂/SiO₂/Si(100) substrates by spin coating at 5000 rpm for 30 s using the precursor solution described above. It was then placed on a hot-plate at ~200 °C for 5 min to remove water and, in a final step, pyrolyzed in an electric furnace (Furnace EDG 1800, The Mellen Company Inc., Concord, NH, USA) at 300 °C for 10 min. The same procedure was repeated on the previously annealed film to increase the film thickness. Finally, the films were crystallized in an electric furnace in air at 700 °C for 30 min. The thickness of the final films was ~500 nm. Circular Au top electrodes of 500 μm in diameter were sputtered on the film surfaces using a shadow mask, thus forming capacitor structures with the Pt bottom electrode. Fig. S1 in the supplementary material summarizes the dielectric, ferroelectric, and conductivity measurements for the studied ($\text{Pb}_{0.88}\text{La}_{0.12}$)($\text{Zr}_{0.52}\text{Ti}_{0.48}$) O_3 thin film. Fig. S2 and S3 in the supplementary material presents a detailed analysis to clarify the relaxor ferroelectric nature of the studied PLZT12 film. In addition, information on the leakage current and conduction mechanisms are summarized in Fig. S4 (supplementary

material). A transmission electron micrograph of the cross-section of a representative part of the thin film is presented in Fig. S5 of the supplementary material showing a columnar-like growth. The thin film is, however, only weakly textured with rocking curves of the order of tens of degrees.

Time-resolved X-ray diffraction of the piezoelectric strain response of the PLZT12 thin film was also performed at the XPP end station of the KMC-3 beamline [33] at the synchrotron BESSY II in Berlin (Germany). A single Au electrode was contacted electrically using a tungsten tip with a tip size $< 5 \mu\text{m}$. PUND (Positive-Up Negative-Down) pulse sequences [34] were applied with frequencies ranging from 15 to 100 kHz and voltages of up to 23 V (corresponding to an electric field of $E = 460 \text{ kV/cm}$) using a home-built voltage amplifier. The sample was glued using conductive silver paint to a metallic sample holder that was connected to the ground. To ensure that the footprint of the incident 9 keV X-ray beam illuminated the contacted electrode exclusively and thus probed only the volume that was actuated when applying an electric field, a horizontal slit with a vertical opening of $150 \mu\text{m}$ was installed 15 cm in front of the sample. The intensity of the diffracted X-rays was measured using a scintillator (Scionix) with a decay time of $< 2 \text{ ns}$ coupled to a photomultiplier (PicoQuant PMA) that was connected to a single photon counting module (PicoQuant PicoHarp300), which enables an optimum time-resolution of 4 ps. In order to increase the signal-to-noise ratio, several channels of the PicoHarp module were binned, thus reducing the effective temporal resolution to $\sim 80 \text{ ns}$. The angle of incidence of the X-rays was set to 15° and the Bragg diffraction peak was measured by performing 2θ scans of the detector angle. The diffraction yield of the 2θ scans for each binned channel of the PicoHarp was fitted using a pseudo-Voigt function from which the 2θ position of the Bragg reflection and the peak width were inferred.

For all X-ray diffraction measurements, the strain was determined from the displacement of the Bragg reflection in 2θ as a function of the applied electric field. The fixed incident angles were chosen so that the probed lattice planes are parallel or slightly inclined by few degrees with respect to the thin film surface. Considering the full width at half maximum (FWHM) of the rocking curve and the displacement of the Bragg peak as a function of the applied electric field, which is much smaller than

the FWHM, 2θ -scans are sufficient using a point detector or, in the case of a 2D detector, no movements are necessary to measure the displacement of the Bragg peak that provides direct access to the induced strain using Bragg's law: Using the lattice constant, a , the strain is defined as $\varepsilon(E) = (a(E) - a(E = 0)) / a(E = 0)$ and $\varepsilon(E) = (a(t) - a(t = 0)) / a(t = 0)$ where E is the applied electric field and t is the time after the start of the PUND sequence, respectively. When taking into account an incidence angle of 10° and a 2θ diffraction angle of 25° for the investigated diffraction peak the normal to the investigated planes lie at $\psi = 5^\circ$ from the surface normal. Considering that strain varies as $\sin^2\psi$ the relative error on the strain with respect to an exactly $\psi = 0$ measurement is of less than 1 %.

Results and discussion

The strain transient for a PLZT12 thin film measured by time-resolved X-ray diffraction at the PLZT 110 Bragg peak during the application of PUND pulse sequences with a frequency of 30 kHz and maximum voltages ranging from +/-15 to +/-23 V is presented in Fig. 1. We note that for all applied voltages, the induced strain is always larger for the negative pulses than for the positive pulses indicating a built-in electric field. These findings are in agreement with *in situ* X-ray diffraction on the same thin film during the application of DC and AC electric fields with frequencies of up to 62.5 Hz that are presented in Fig. S6 in the supplementary material and which are similar to the results reported in ref. [32]. The strain increases, particularly for negative voltage pulses, with increasing applied voltage agreeing with the inverse piezoelectric effect: $\varepsilon_3 = d_{33}E_3$. The piezoelectrically-induced strain for $U = 15$ V (electric field of $E = 300$ kV/cm) is similar to the strain obtained during AC measurements shown in Fig. S6 and Fig. S7 of the supplementary material despite the considerably higher frequency of 30 kHz as compared to 62.5 Hz. The piezoelectric coefficient d_{33} for the positive and the negative polarities amounts to 11 and 14 pm/V, respectively, compared to 10 and 17 pm/V at 62.5 Hz.

The Bragg peak width Δq , which is a measure of the disorder in the material (neglecting finite size contributions), is shown in Fig. 1(b) for the three different applied voltages. The variation of Δq increases with increasing applied electric field. Considering that the grain size is not affected by

applying an electric field, the peak width variations are caused by strain distribution and the orientation of domains. The peak width always increases for positive electric fields suggesting incomplete switching of ferroelectric domains due to the built-in electric field. In contrast, the decreasing peak width for negative pulses indicates polarization reversal.

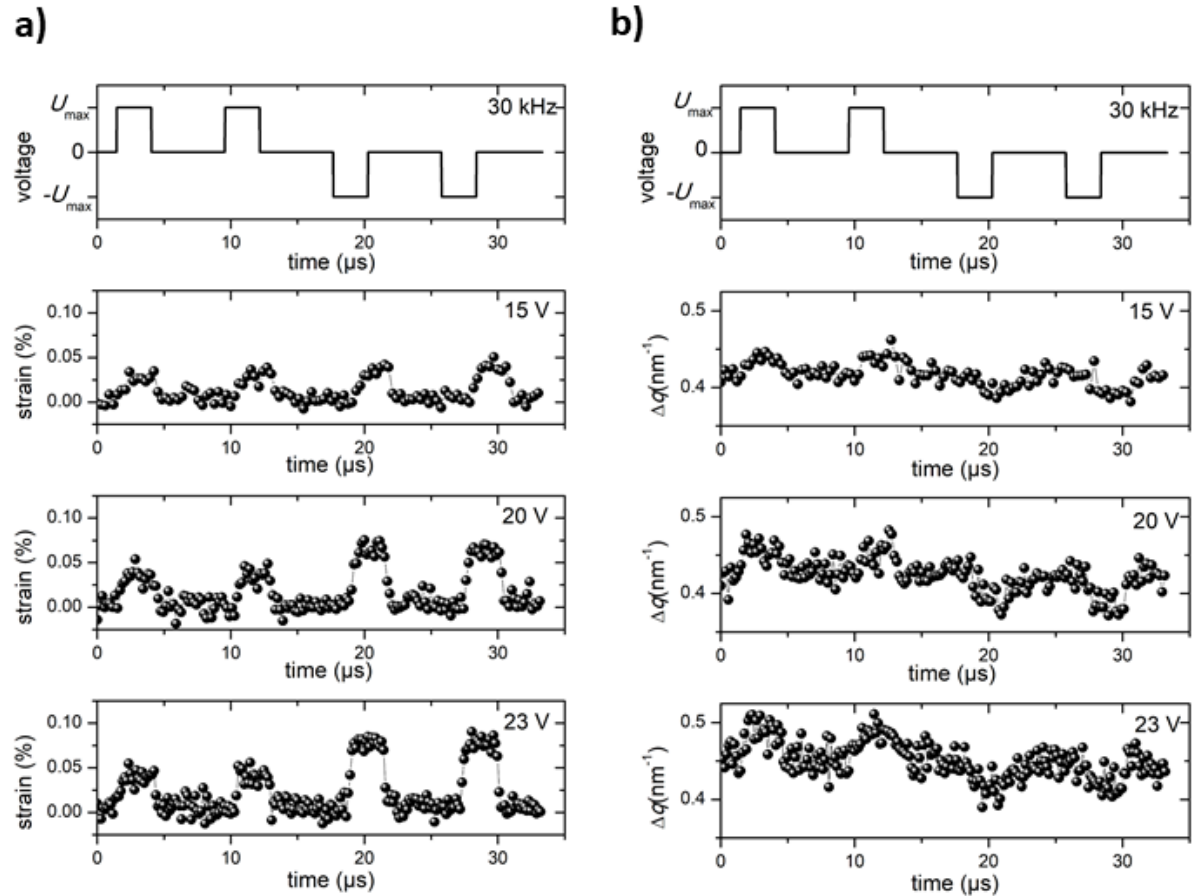


Fig. 1: a) Strain transient and b) transient of the peak width Δq of the PLZT 110 Bragg reflection for a PUND pulse sequence with a frequency of 30 kHz and peak voltages of 15, 20, and 23 V. Additional frequencies of 15, 60, and 100 kHz for the three different voltages of 15, 20, and 23 V are shown in Fig. S9 of the supplementary material.

The strain transient and the transient of the Bragg peak width measured at the PLZT 110 Bragg peak of the PLZT12 thin film during the application of PUND pulses sequences with a maximum voltage of +/- 23 V (electric field of $E = 460$ kV/cm) and frequencies ranging from 15 to 100 kHz are presented

in Fig. 2(a) - (d). The imprint effect is visible for all frequencies measured in this work showing larger strain for negative polarity pulses than for positive polarity pulses. The asymmetry observed in the current density $J(E)$ curve shown in Fig. S4(a) of the supplementary material reinforces the imprint effect in the studied film. In addition, the analysis on the conduction mechanisms presented in Fig. S4(b), (c), and (d), indicate that the space-charge limited current (SCLC), Schottky (SC) emission and the Fowler-Nordheim (FN) tunneling mechanisms dominate at low, intermediate, and high electric fields, respectively. While the strain reaches a constant value for electric field pulses at the frequencies 15, 30, and 60 kHz, this is not the case for the 100 kHz measurement, indicating that the time needed for the polarization saturation is longer than the applied voltage pulse duration of $\sim 1 \mu\text{s}$. In addition, for the highest applied frequency (100 kHz), the strain value is larger for the non-switching pulses (*i.e.* the second positive and second negative pulse), compared to the switching pulses (first positive and first negative pulse), which is not reflected in the peak width change. One might expect a reduced piezoelectric strain formation due to the high repetition rate of the experiment with short periods of the applied field.

In general, the Bragg peak width is always larger for the positive pulses while it decreases for the negative ones. Therefore, a larger Δq indicates a more significant disorder and, thus, many incompletely switched ferroelectric domains. At the same time, the decreasing peak width for negative pulses indicates switching of the domains even when the saturation polarization has not been achieved yet, as also inferred from the transient strain response. These findings are in good agreement with the presence of a built-in electric field in the thin film that reduces the effectively applied electric field for positive pulses and enhances the efficiency of the applied negative pulses. The lower effective field for positive pulses leads to an incomplete switching of the domains. It should be noted that the variation of the peak width is significantly smaller at 60 kHz and 100 kHz compared to lower frequencies.

The switching of ferroelectric domains affects the structure factor of the material, changing the diffracted intensity [22]. For high frequencies (60 and 100 kHz), the Bragg peak intensity decreases by about 4% in case of electric field pulses with positive polarity while it remains unchanged for negative

This is the author's peer reviewed, accepted manuscript. However, the online version of record will be different from this version once it has been copyedited and typeset.
PLEASE CITE THIS ARTICLE AS DOI: 10.1063/1.50077785

polarity. This decrease in the integrated diffraction intensity for positive polarity in case of high frequencies signifies a change in the structure factor which originates from a switching of the ferroelectric domains. A long-lasting intensity difference of $\sim 1\%$ is observed in between the switching and non-switching pulses indicating that only a negligible fraction of the sample reversed its polarity during the application of the pulses with positive polarity. The fact that the intensity returns to its initial value in between the electric field pulses further indicates that the remanent polarization is small compared to the polarization under electric field. That the integrated diffracted intensity does not vary for pulses with negative polarity is probably caused by a pre-poling of the sample during the alignment process where a DC potential was applied. These findings are in agreement with the previously discussed transient peak width changes and again emphasize that the built-in field heavily affects the switching dynamics of the film and only the positive PUND pulses lead to a change of the domain state. For lower frequencies no variation of the integrated diffraction intensity is apparent which is probably due to the comparatively high noise of more than 5%. Considering a coercive field of about 10 V as demonstrated by Fig. S8 in the supplementary material compared to 23 V applied during the PUND pulse sequences, the switching behavior of the ferroelectric domains is, however, surprising and deserves more investigation in the future, in particular, for PUND electrical measurements.

This is the author's peer reviewed, accepted manuscript. However, the online version of record will be different from this version once it has been copyedited and typeset.
PLEASE CITE THIS ARTICLE AS DOI: 10.1063/1.5007785

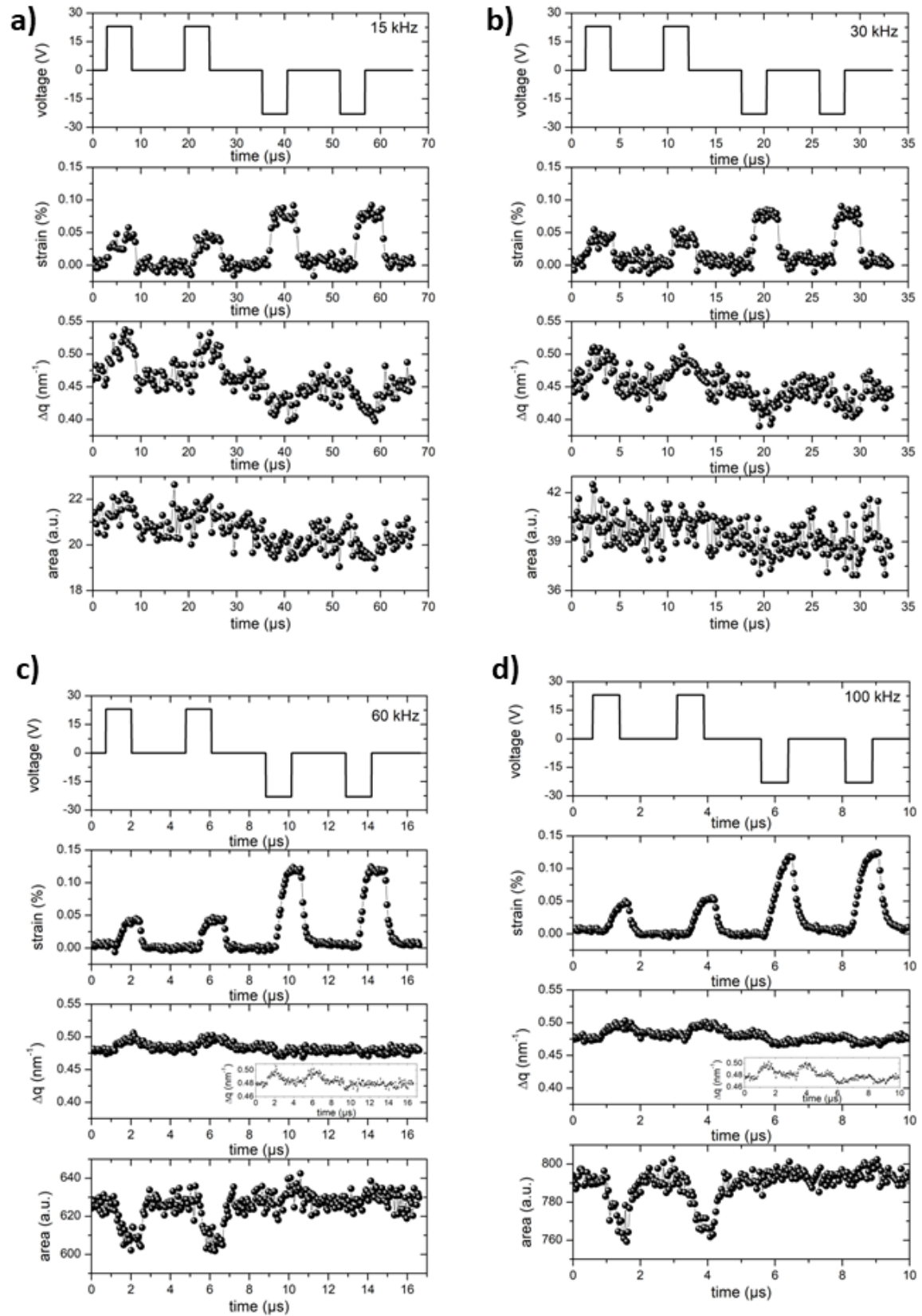


Fig. 2: Strain transient, transient of peak width, and transient of the integrated diffraction intensity measured at the PLZT 110 Bragg peak for a PLZT12 thin film during the application of PUND pulse

sequences with a maximum voltage of ± 23 V ($E = \pm 460$ kV/cm) at a frequency of a) 15 kHz, b) 30 kHz, c) 60 kHz, and d) 100 kHz. Insets in (c) and (d) show the variation of the peak width at 60 Hz and 100 kHz on a magnified scale to improve the visibility of the variations.

From the fitting of the increasing and decreasing flanks of the strain transient for each pulse with an exponential function (which is presented in Fig. S10 of the supplementary material), we determine the characteristic times for polarization and depolarization of the ferroelectric relaxor thin film. The inferred time constants are listed in Table 1 and presented in Fig. 3. The decay times (OFF) are, in general, significantly smaller than the rising times (ON). Moreover, the rising time of the switching pulses (first and third pulse) is always by a factor of about 1.5 longer than for the non-switching pulses (second and fourth pulse) and a factor of 2 to 3 longer than the decay times. The characteristic time and the uncertainties increase significantly for frequencies of 30 and 15 kHz. This originates from the fact that the complete pulse sequence is measured with the same number of channels at the higher frequencies (hence a shorter period). Thus, a smaller number of channels of the PicoHarp probes the increasing and decreasing flanks, hence significantly increasing the fitting uncertainty.

Table 1: Time constants in nanoseconds of the strain transient for the increasing (ON) and decreasing (OFF) flanks for the four different pulses of PUND pulse sequence with frequencies of 15, 30, 60, and 100 kHz.

		100 kHz	60 kHz	30 kHz	15 kHz
ON	1 st pulse	278 ± 69	318 ± 56	434 ± 161	720 ± 381
	2 nd pulse	229 ± 38	203 ± 22	119 ± 63	500 ± 222
	3 rd pulse	450 ± 92	293 ± 26	268 ± 36	577 ± 126
	4 th pulse	355 ± 63	219 ± 21	216 ± 40	465 ± 83
OFF	1 st pulse	116 ± 8	106 ± 10	113 ± 61	381 ± 139
	2 nd pulse	113 ± 7	99 ± 10	283 ± 130	304 ± 118
	3 rd pulse	149 ± 4	180 ± 11	122 ± 36	487 ± 116
	4 th pulse	138 ± 3	177 ± 10	107 ± 27	373 ± 57

This is the author's peer reviewed, accepted manuscript. However, the online version of record will be different from this version once it has been copyedited and typeset.
PLEASE CITE THIS ARTICLE AS DOI: 10.1063/1.50077785

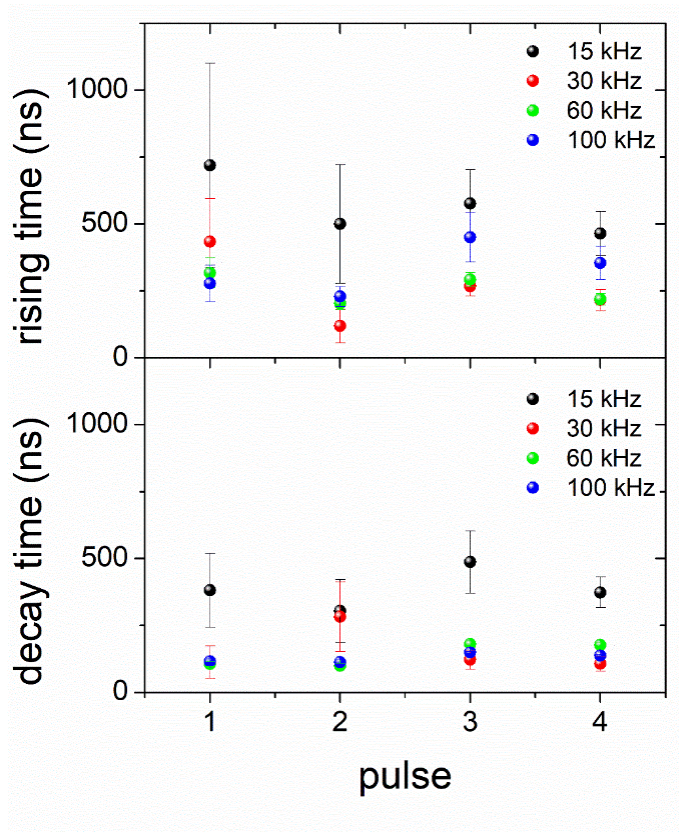


Fig. 3: Time constants for a) the increasing and b) the decreasing strain response of the PLZT12 thin film during the application of PUND pulse sequences with frequencies ranging from 15 to 100 kHz.

Discussion

The shift of the maximum of the real part of the dielectric permittivity (ϵ') to higher temperatures with the increase of the frequency and the slim ferroelectric hysteresis loop (shown in Fig. S1(b) and Fig. S1(c) of the supplementary material, respectively), indicate characteristics of relaxor ferroelectrics as the studied PLZT12 film. Although the subtle temperature-frequency-dependent peak of the dielectric permittivity may not be clear in Fig. S1(b) or hidden by interfacial effects at low frequencies, the frequency as a function of the temperature of maximum permittivity (T_{max}) of the studied film shown in Fig. S2 evidences the temperature-frequency dispersion of the dielectric permittivity with a freezing temperature $T_f = 385$ K. Fig. S3(a) and S3(b) give additional information on the relaxor nature of the studied PLZT12 thin film. From data in Fig. S3(b), the obtained diffuseness parameter $\gamma = 1.93$ value characterizes a diffuse transition for the studied $(\text{Pb}_{0.88}\text{La}_{0.12})(\text{Zr}_{0.52}\text{Ti}_{0.48})\text{O}_3$ thin film.

Different effects are observed when applying an electric field pulse sequence such as the PUND sequence described above. Supposing that the electric field is larger than the coercive field, the first and third applied pulses induce both ferroelectric domains switching and charging of the capacitor formed by the top electrode/PLZT12/bottom electrode. The capacitor will only be charged during the second and fourth voltage pulses, but in principle, no domain switching should occur. However, the ferroelectric is partially repolarized since the polarization is reduced to the remanent value when no electric field is applied. Therefore, the switching pulses contain the temporal behavior of the switching process of the domains and the charging time of the capacitor, which are the quantities most relevant for commercial applications. The capacitor discharges when switching off the external electric field, and the polarization decreases to its remanent value. Hence, the characteristic time when turning off the electric field is the relaxation time $\tau = R \cdot C$ of the RC circuit. Considering a thickness of 500 nm for the ferroelectric thin film, a diameter of 500 μm of the top Au electrodes, and dielectric permittivity of 240 (as measured on a PLZT12 thin film at 100 kHz at room temperature (Fig. S1(b))), the capacitance is of the order of 0.8 nF. A characteristic time of the order of 50 ns is expected for the RC circuit taking into account the electrical resistance of the connecting cables of a few Ohms as well as a 50 Ω termination resistor, which is close to the minimum switching time found in other works for samples with similar composition and smaller contact pads [35]. It is smaller than the measured characteristic time scales and thus does not limit the experiment even at high frequencies. The switching times found in our experiments on PLZT are comparable to results found in other experiments on PZT thin films of various compositions with switching times between 600 ps and 10 ms [36, 37, 38]. The fact that the characteristic time when applying an electric field τ_{on} is always significantly larger than τ_{off} when switching off the external electric field clearly reflects the temporal evolution of the polarization and the structural response of the relaxor thin film. The larger τ_{on} of the non-switching pulses compared to τ_{off} might originate from partial repolarization of the ferroelectric and a partial misorientation of the polarization. that we attribute to the presence of polar nanoregions in the context of the built-in electric field found in our sample and comparable sample heterostructures [29,30]. This is in

agreement with the integrated diffraction intensity returning to its initial value in between the electric field pulses signifying a low remanent polarization as also demonstrated by the slim P-E curves, which are signs of a relaxor behavior.

The characteristic time for the switching of the ferroelectric domains τ_{switch} is determined from the switching pulses by subtracting the characteristic time when turning off the applied external field from the one when applying the electric field resulting in τ_{switch} of the order of 100 to 200 ns. This characteristic time is comparable to switching times derived from the measurement of the transient switching current in, e.g., reference [37] for epitaxial PZT thin film heterostructures. The imaginary part of the dielectric permittivity increases reaching the MHz range, which agrees with a time constant of a few hundred nanoseconds. However, the measurement range of the applied frequency is not sufficient to determine the peak of the dielectric permittivity expected for a relaxor ferroelectric.

The typical velocity of domain walls in ferroelectric thin films is of the order of 1 m/s [39]. However, the time scales for polarization switching may span from hundreds of picoseconds to milliseconds [40] depending on the physical size of ferroelectric capacitors, the microstructure of the ferroelectric, the temperature, and the magnitude of an applied electric field, amongst others. The time of polarization switching decreases exponentially with the increasing magnitude of an applied electric field [41]. We emphasize here that the present work is, to our knowledge, the first time that polycrystalline thin films were investigated using time-resolved X-ray diffraction. The difference in the dynamics comparing crystalline and polycrystalline samples with and without relaxor properties show that the timescale for the polarization reversal is comparable. However, the built-in electrical field significantly affects the timing for different polarities, proving that such materials are useful due to their piezoelectric properties. Future studies will focus on the influence of La concentration ranging from pure PZT up to the relaxor composition to study further the transition of the lanthanum modified PZT thin film from a ferroelectric to a relaxor ferroelectric material and further elucidate the effect of polar nanoregions in relaxors.

Conclusion

In conclusion, time-resolved X-ray diffraction was performed on lanthanum-modified PZT relaxor thin films evidencing a built-in electric field that is oriented from the top to the bottom electrode. The application of PUND pulse sequences with frequencies of up to 100 kHz demonstrates a longer time response for the switching pulses than the non-switching pulses, related to the domain switching in the relaxor ferroelectric. In addition, the Bragg peak width was found to be larger for positive applied pulses than for negative ones, which is attributed to the incomplete switching of ferroelectric domains due to the built-in electric field. The transient of the integrated diffraction intensity confirms this incomplete switching and indicates a low remanent polarization in agreement with polarization-electric field curves typical for relaxor ferroelectrics. Considering a coercive field of 10 V in comparison to 23 V that are applied during PUND pulse sequences, the switching behavior of the ferroelectric domains is surprising and deserves more investigations. From the time-resolved measurements, the characteristic time for switching the ferroelectric domains in the PLZT12 thin film was determined to be 100 to 200 ns. These characteristic times for a polycrystalline thin film are comparable to epitaxial PZT thin films of various compositions. However, the built-in electric field significantly affects the timing for different polarities, which proves that such materials are useful due to their piezoelectric properties.

Supplementary Material

The supplementary material contains measurements of the dielectric permittivity, conductivity and ferroelectric properties of the studied PLZT12 thin film. The relaxor characteristics of the studied PLZT thin film are characterized and an analysis on the leakage current density and the conductivity mechanisms are given. It further shows a transmission electron micrograph of the cross-section of the thin film revealing its columnar growth. In addition, *in situ* X-ray diffraction results obtained during the application of DC and AC electric fields are presented showing asymmetric butterfly loops. The maximum piezoelectrically-induced strain as well as the ratio of the strain for positive and negative

polarity measured by *in situ* X-ray diffraction are presented as well as the variation of the integrated diffraction intensity and the full width at half maximum of the PLZT 110 Bragg reflection during the application of DC voltages. It further includes additional time-resolved X-ray diffraction data taken at different frequencies of PUND pulse sequences with different maximum voltages. The fitting of the rising and falling flanks of the strain transients by an exponential function is further illustrated showing the fitting quality.

Acknowledgements

The authors gratefully acknowledge the SOLEIL Synchrotron for allocating beam time. Detector and Electronics Support Groups, as well as P. Joly, are acknowledged for excellent technical support during the experimental campaign at SOLEIL Synchrotron on DiffAbs beamline. We further thank the BESSY program committee for allocating beamtime at the KMC3-XPP beamline and Wolfram Leitenberger from the University of Potsdam for experimental support during the initial stage of the project. This research was supported by the Fundação de Amparo à Pesquisa do Estado de São Paulo, FAPESP (Project: 2017/13769-1) and Coordenação de Aperfeiçoamento de Pessoal de Nível Superior, CAPES (CAPES-PRINT Project: 88881.310513/2018-01). Also, we would like to express our gratitude to the CAPES-COFECUB (Project N° 801-14) for their financial support.

References

1. Martin, L.W.; Rappe, A.M. *Thin-film ferroelectric materials and their applications*, Nature Rev. Materials 2 (2017) 16087
2. Damjanovic, D.; Newnham, R.E. *Electrostrictive and Piezoelectric Materials for Actuator Applications*, J. Intell. Mater. Syst. Struct., 3 (1992) 190–208
3. Damjanovic, D. *Hysteresis in piezoelectric and ferroelectric materials*. In The Science of Hysteresis, 3 (2006) 337–465

4. Noheda, B.; Cox, D.E.; Shirane, G.; Gonzalo, J.A.; Cross, L.E.; Park, S.-E. *A monoclinic ferroelectric phase in the $Pb(Zr_{1-x}Ti_x)O_3$ solid solution*, Appl. Phys. Lett. 74 (1999) 2059.
5. Noheda, B.; Gonzalo, J.A.; Cross, L.E.; Guo, R.; Park, S.E.; Cox, D.E.; Shirane, G. *Tetragonal-to-monoclinic phase transition in a ferroelectric perovskite: The structure of $PbZr_{0.52}Ti_{0.48}O_3$* , Phys. Rev. B 61 (2000) 8687.
6. Sahoo, B.; Panda, P.K. *Effect of lanthanum, neodymium on piezoelectric, dielectric and ferroelectric properties of PZT*, J. Adv. Ceramics 2 (2013) 37-41
7. Zou, Q.; Ruda, H.; Yacobi, B.; Farrell, M. *Microstructural characterization of donor-doped lead zirconate titanate films prepared by sol-gel processing*, Thin Solid Films 402 (2002) 65-70
8. Aggarwal, S.; Ramesh, R. *Point defect chemistry of metal oxide heterostructures*, Ann. Rev. Mater. Sci. 28 (1998) 463.
9. Lines, M.E.; Glass, A.M., *Principles and Applications of Ferroelectrics and Related Materials*, Clarendon, Oxford (1977).
10. Burns, G.; Dacol, F.H. *Crystalline ferroelectrics with glassy polarization behaviour*, Phys. Rev. B 28 (1983) 2527–2530
11. Cross, L.E. *Relaxor ferroelectrics*, Ferroelectrics 76 (1987) 241-267.
12. Cohen, R. E. *Relaxors go critical*, Nature 441 (2006) 941-942.
13. Fu, H.; Cohen, R.E. *Polarization rotation mechanism for ultrahigh electrochemical response in single-crystal piezoelectrics*, Nature 403 (2000) 281
14. Park, S.E.; Shrout, T.R. *Ultrahigh strain and piezoelectric behavior in relaxor based ferroelectric single crystals*, J. Appl. Phys. 82 (1997) 1804-1811
15. Kholkin, A.; Morozovska, A.; Kiselev, D.; Bdikin, I.; Rodriguez, B.; Wu, P.; Bokov, A.; Ye, Z.-G.; Dkhil, B.; Chen, L.-Q.; Kosec, M.; Kalinin, S.V. *Surface domain structure and mesoscopic phase transition in relaxor ferroelectrics*, Adv. Func. Mat. 21 (2011) 1977.
16. Haertling, G.H. *Ferroelectric Ceramics: History and Technology*, J. Am. Ceram. Soc. 82 (1999) 797.

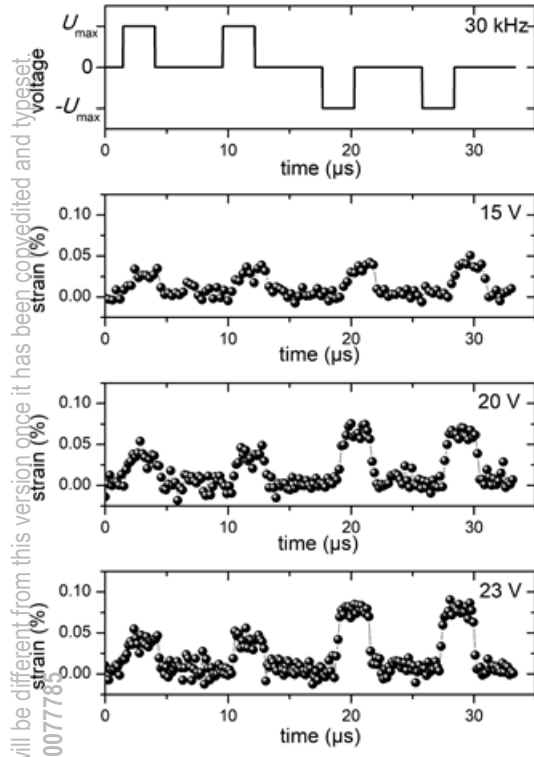
17. Poosanaas, P; Uchino, K. *Photostrictive effect in lanthanum-modified lead zirconate titanate ceramics near the morphotropic phase boundary*, Mater. Chem. Phys. 61 (1999) 36.
18. Kholkin, A.L.; Wütchrich, Ch.; Taylor, D.V.; Setter, N. *Interferometric measurements of electric field-induced displacements in piezoelectric thin films*, Rev. Sci. Instrum. 67 (1996) 1935.
19. Young, J.; Chen, P.; Sichel, R.J.; Callori, S.J.; Sinsheimer, J.; Dufresne, E.M.; Dawber, M.; Evans, P.G. *Nanosecond dynamics of ferroelectric/dielectric superlattices*, Phys. Rev. Lett. 107 (2011) 055501.
20. Gorfman, S.; Simons, H.; Iamsasri, T.; Prasertpalichat, S.; Cann, D.P.; Choe, H.; Pietsch, U.; Watter, Y.; Jones, J.L. *Simultaneous resonant x-ray diffraction measurement of polarization inversion and lattice strain in polycrystalline ferroelectrics*, Sci. Rep. 6 (2016) 20829.
21. Pramanick, A.; Damjanovic, D.; Daniels, J.E.; Nino, J.C.; Jones, J.L. *Origins of electro-mechanical coupling in polycrystalline ferroelectrics during subcoercive electrical loading*, J. Am. Ceram. Soc. 94 (2011) 293-309
22. Gorfman, S.; Schmidt, O.; Tsirelson, V.; Ziolkowski, M.; Pietsch, U. *Crystallography under external electric field*, Z. Anorg. Allg. Chem. 639 (2013) 1953-1962
23. Wooldridge, J.; Ryding, S.; Brown, S.; Burnett, T.L.; Cain, M.G.; Cernik, R.; Hino, R.; Stewart, M.; Thompson, P. *Simultaneous measurement of X-ray diffraction and ferroelectric polarization data as a function of applied electric field and frequency*, J. Synchrotron Radiat. 19 (2012) 710
24. Nguyen K.; Bellec, E.; Zatterin, E.; Le Rhum, G.; Gergaud, P.; Vaxelaire, N., *Structural insights of electrical aging in PZT thin films as revealed by in situ biasing X-ray diffraction*, Materials 14 (2021) 4500
25. Kwamen, C.; Rössle, M.; Leitenberger, W.; Alexe, M.; Bargheer, M. *Time-resolved X-ray diffraction study of the structural dynamics in an epitaxial ferroelectric thin $Pb(Zr_{0.2}Ti_{0.8})O_3$ film induced by sub-coercive fields*, Appl. Phys. Lett. 114 (2019) 162907
26. Fancher, C.M.; Choe, H.; Gorman, S.; Simons, H.; Chung, C.C.; Ziolkowski, M.; Prasertpalichat, S.; Cann, D.P.; Jones, J.L. *Effect of alloying $BaTiO_3$ with $BiZn_{1/2}Ti_{1/2}O_3$ on polarization reversal*, Appl. Phys. Lett. 117 (2020) 042907

27. Davydok, A.; Cornelius, T.W.; Mocuta, C.; Lima, E.C.; Araùjo, E.B.; Thomas, O. *In situ X-ray diffraction studies on the piezoelectric response of PZT thin films*, Thin Solid Films 603 (2016) 29-33
28. Lee, K.S.; Kim, Y.K.; Baik, S.; Kim, J.; Jung, I.S. *In situ observation of ferroelectric 90°-domain switching in epitaxial Pb(Zr,Ti)O₃ thin films by synchrotron X-ray diffraction*, Appl. Phys. Lett. 79 (2001) 2444.
29. Baturin, I.; Menou, N.; Shur, V.; Muller, C.; Kuznetsov, D.; Hodeau, J.L.; Sternberg, A. *Influence of irradiation on the switching behavior in PZT thin films*, Materials Science and Engineering B 120 (2005) 141-145.
30. Cao, J.L.; Zhang, K.; Solbach, A.; Yue, Z.; Wang, H.H.; Chen, Y.; Klemradt, U. *In situ X-ray reflectivity study of imprint in ferroelectric thin films*, Materials Science Forum 687 (2011) 292-296.
31. Kwamen, C.; Rössle, M.; Reinhardt, M.; Leitenberger, W.; Zamponi, F.; Alexe, M.; Bargheer, M. *Simultaneous dynamic characterization of charge and structural motion during ferroelectric switching*, Phys. Rev. B 96 (2017) 134105
32. Cornelius, T.W.; Mocuta, C.; Escoubas, S.; Lima, L.R.M.; Araùjo, E.B.; Kholkin, A.L.; Thomas, O. *Piezoelectric properties of Pb_{1-x}La_x(Zr_{0.52}Ti_{0.48})O₃ thin films studied by in situ X-ray diffraction*, Materials 13 (2020) 3338
33. Rössle, M.; Leitenberger, W.; Reinhardt, M.; Koç, A.; Pudell, J.; Kwamen, C.; Bargheer, M. *The time-resolved hard X-ray diffraction endstation KMC-3 XPP at BESSY II*, J. Synchrotron Radiat. 28 (2021) 948–960.
34. Setter, N.; Damjanovic, D.; Eng, L.; Fox, G.; Gevorgian, S.; Hong, S.; Kingon, A.; Kohlstedt, H.; Park, N.Y.; Stephenson, G. B.; Stolitchnov, I.; Taganstev, A. K.; Taylor, D.V.; Yamada, T.; Streiffer, S. *Ferroelectric thin films: Review of materials, properties, and applications*, J. Appl. Phys. 100 (2006) 051606.
35. Song, T.K.; So, Y.W.; Kim, D.J.; Jo, J.Y.; Noh, T.W. *Ferroelectric switching dynamics and pulse-switching polarization measurements*, Integr. Ferroelectr. 78 (2006) 191–197.

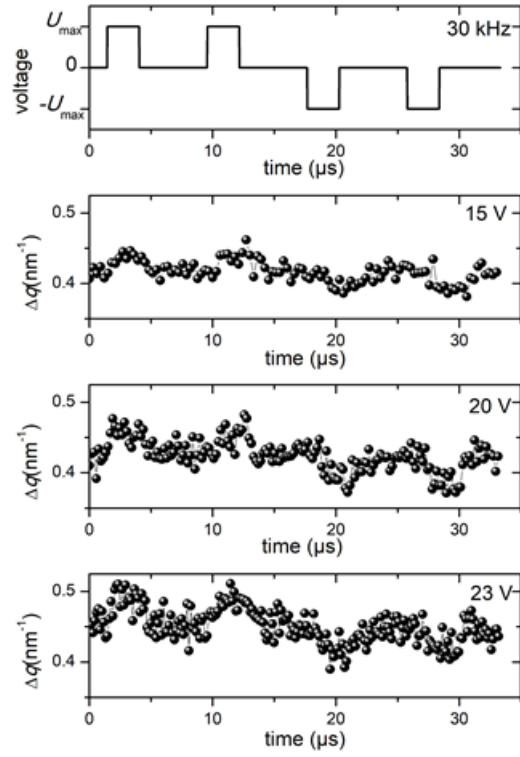
This is the author's peer reviewed, accepted manuscript. However, the online version of record will be different from this version once it has been copyedited and typeset.
PLEASE CITE THIS ARTICLE AS DOI: 10.1063/1.50077785

-
36. Scott, J.F. *et al.* *Switching kinetics of lead zirconate titanate submicron thin-film memories*, J. Appl. Phys. 64 (1988) 787–792.
 37. Shur, V. Y. *et al.* *Switching kinetics in epitaxial PZT thin films*, Microelectron. Eng. 29 (1995) 153–157.
 38. So, Y. W., Kim, D. J., Noh, T. W., Yoon, J.-G. G. & Song, T. K. *Polarization switching kinetics of epitaxial $Pb(Zr_{0.4}Ti_{0.6})O_3$ thin films*, Appl. Phys. Lett. 86 (2005) 092905.
 39. Gruverman, A.; Rodriguez, B.J.; Dehoff, C.; Waldrep, J.D.; Kingon, A.I.; Nemanich, R.J.; Cross, J.S. *Direct studies of domain switching dynamics in thin film ferroelectric capacitors*, Appl. Phys. Lett. 87 (2005) 082902
 40. Tagantsev, A.K.; Stolichnov, I.; Setter, N.; Cross, J.S.; Tsukada, M. *Non-Kolmogorov-Avrami switching kinetics in ferroelectric thin films*, Phys. Rev. B 66 (2002) 214109
 41. Merz, W.J. Phys. Rev. 95 (1954) 690

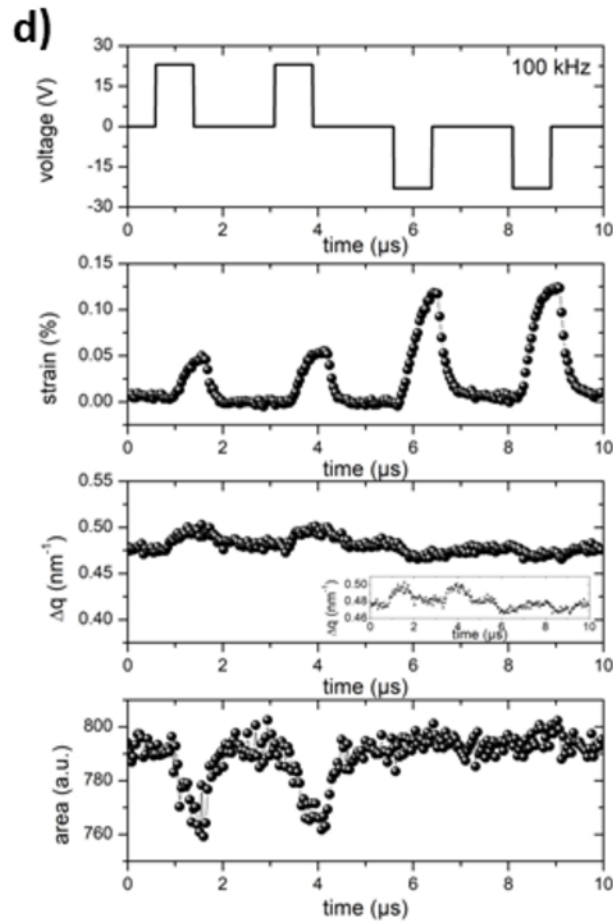
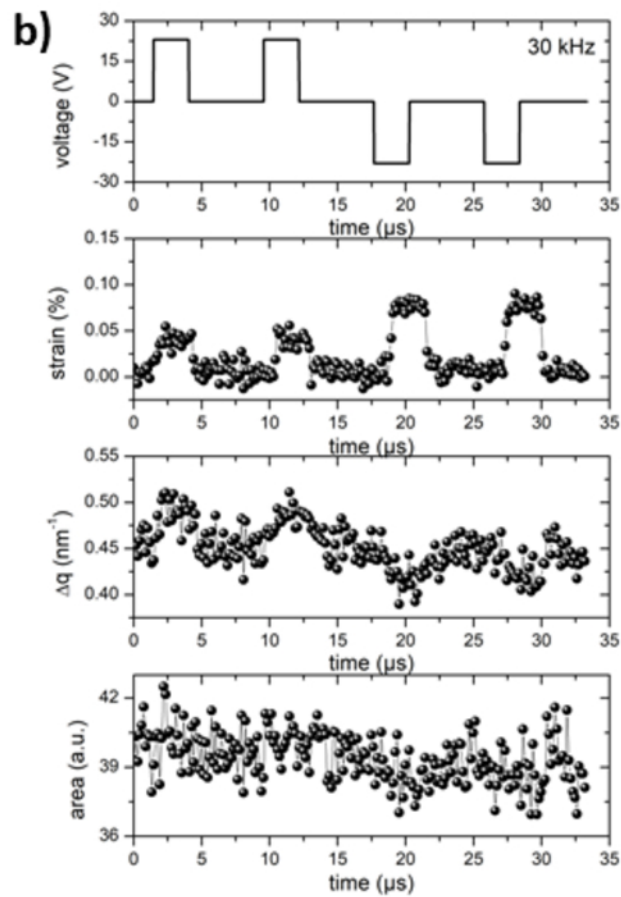
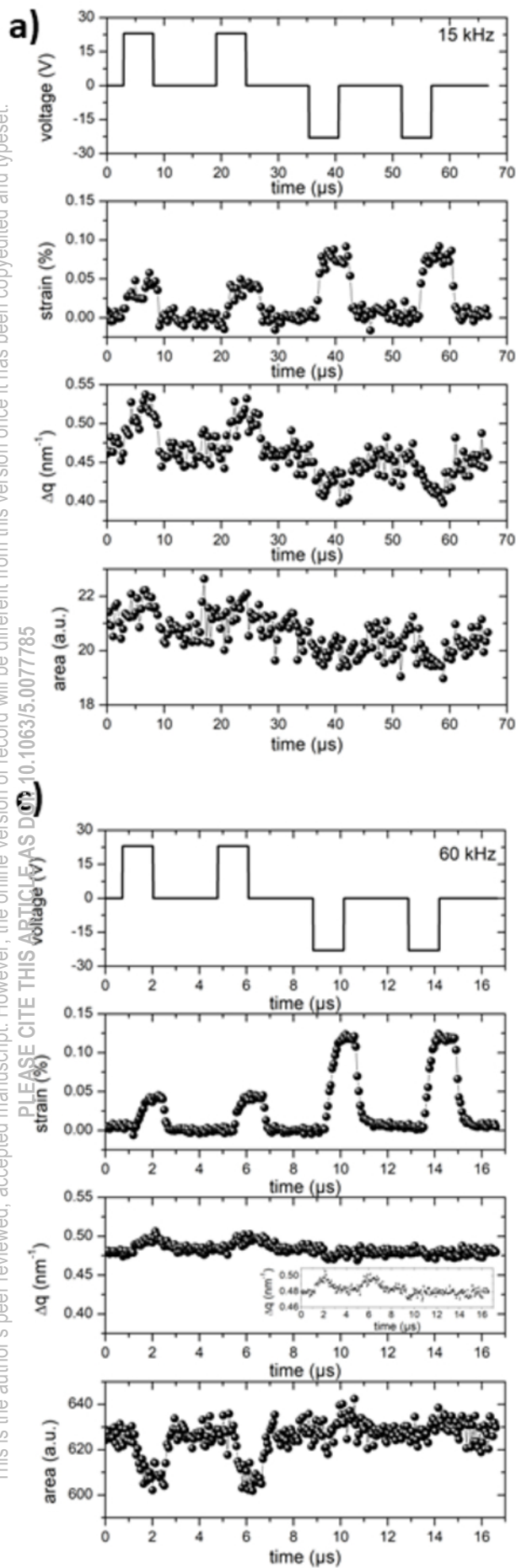
a)



b)



This is the author's peer reviewed, accepted manuscript. However, the online version of record will be different from this version once it has been copyedited and typeset.
PLEASE CITE THIS ARTICLE AS DOI:10.1063/5.0077785



This is the author's peer reviewed, accepted manuscript. However, the online version of record will be different from this version once it has been copyedited and typeset.

decay time (ms) **rising time (ns)**

